

Supporting Information

Red, Yellow, Green, and Blue Amplified Spontaneous Emission and Lasing Using Colloidal CdSe Nanoplatelets

Chunxing She,¹ Igor Fedin,¹ Dmitriy S. Dolzhnikov,¹ Peter D. Dahlberg,⁴ Gregory S. Engel,^{1,5} Richard D. Schaller,^{2,3} and Dmitri V. Talapin^{1,2*}

¹ Department of Chemistry and the James Franck Institute, University of Chicago, Illinois 60637, USA

² Center for Nanoscale Materials, Argonne National Laboratory, Argonne, Illinois 60439, USA

³ Department of Chemistry, Northwestern University, Evanston, IL 60208, USA

⁴ Graduate Program in the Biophysical Sciences, The James Franck Institute, and The Institute for Biophysical Dynamics, The University of Chicago, Chicago, Illinois 60637, USA

⁵ The Institute for Biophysical Dynamics, University of Chicago, Illinois 60637, USA

* E-mail: dvtalapin@uchicago.edu

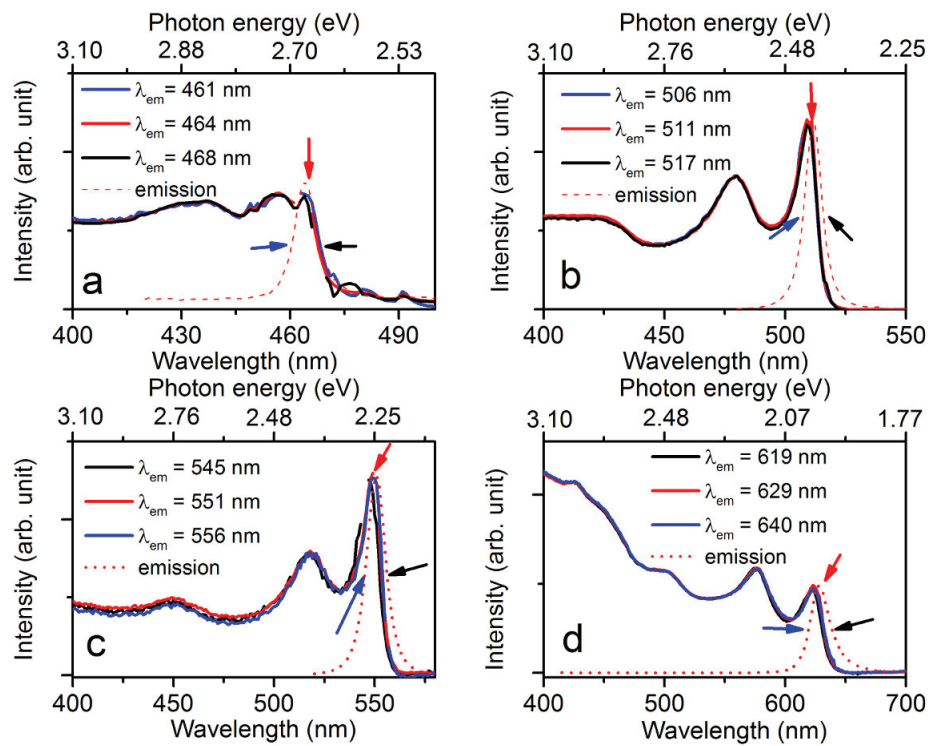


Figure S1. Emission spectrum (dashed line) and Photoluminescence Excitation (PLE) spectra (solid lines) for (a) 3CdSe, (b) 4CdSe, (c) 5CdSe, and (d) 3CdS/4CdSe/3CdS NPLs in hexane. For each sample, PLE spectra were recorded for three different emission wavelengths, indicated by the three arrows; the identical spectra indicate that all NPLs in one ensemble sample have the same thickness.

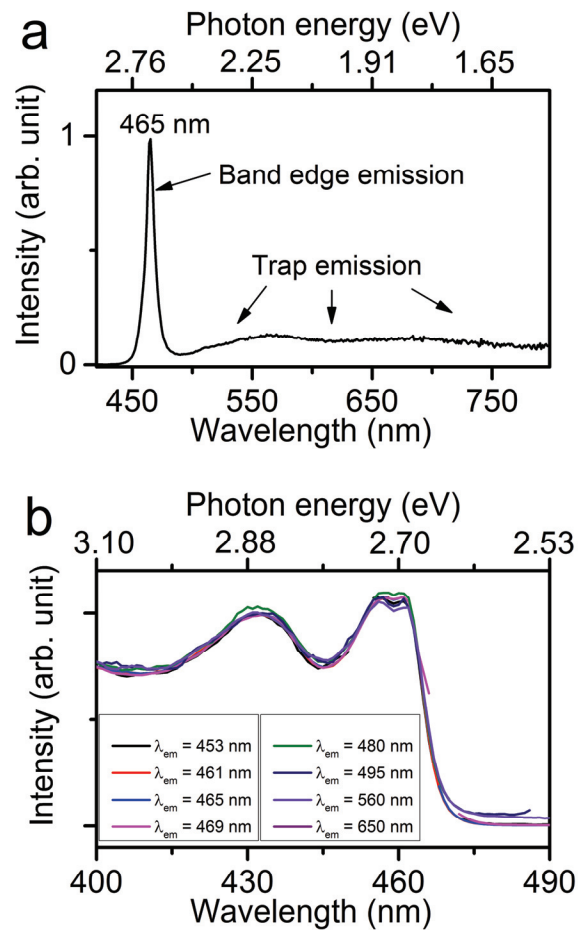


Figure S2. Photoluminescence Excitation (PLE) spectra for 3CdSe NPLs monitored at multiple different emission wavelengths. The identical spectra indicate that the emissions in the long wavelength region come from NPLs with trap states.

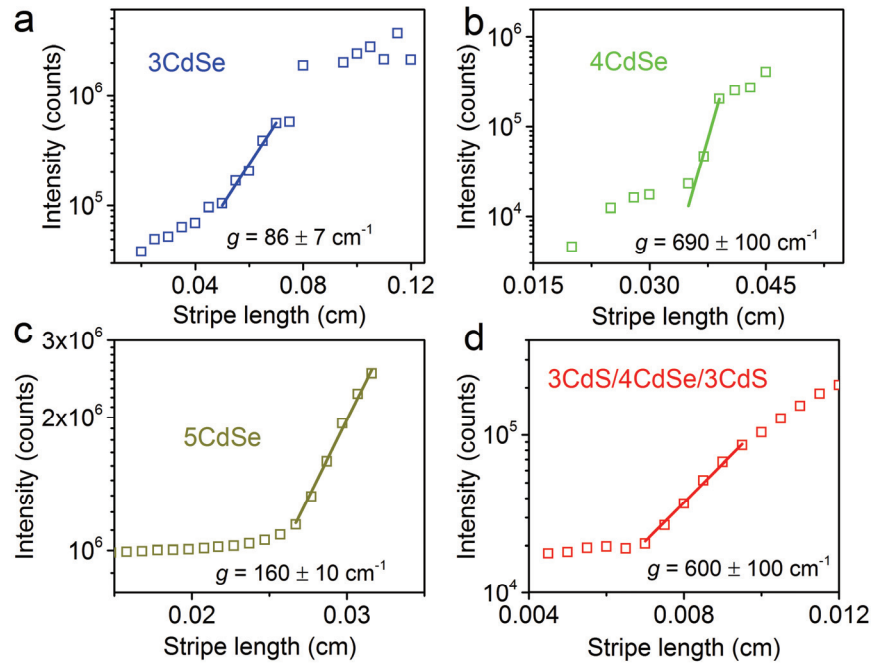


Figure S3. Integrated emission intensity, I , as a function of stripe length, l , from films of (a) 3CdSe, (b) 4CdSe, (c) 5CdSe, and (d) 3CdS/4CdSe/3CdS. The dots are experimental data, and the solid lines are fits to $I = I_0 + A(e^{gl}-1)/g$, where A is a constant proportional to the spontaneous emission power density, and g is the modal gain. Excitation is at 400 nm.

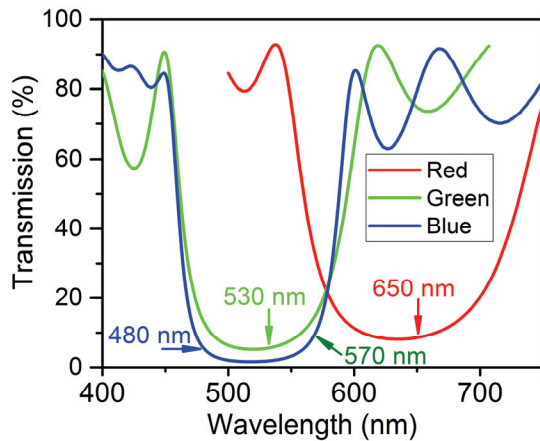


Figure S4. Transmission spectra of the partial reflective mirrors used in the lasing experiments. Arrows indicate the transmission for lasing at different wavelengths.

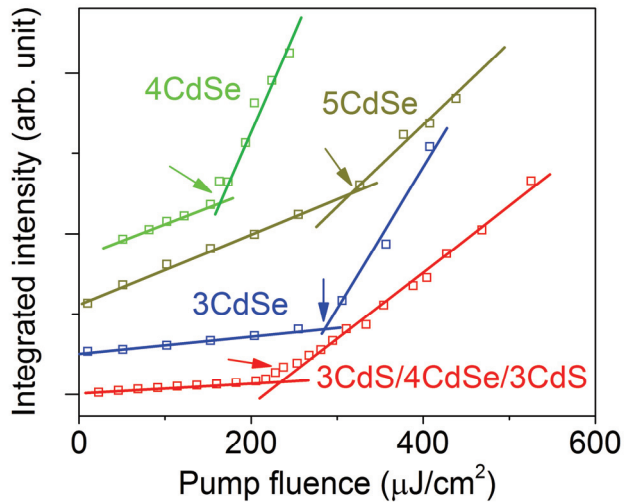


Figure S5. Pump-fluence-dependent total lasing intensities of 3CdSe, 4CdSe, 5CdSe, and 3CdS/4CdSe/3CdS. Excitation is at 400 nm. Dots are experimental data. Solid lines are linear fits to the data in different regions. The arrows point to lasing thresholds, which are 290 $\mu\text{J}/\text{cm}^2$ (3CdSe), 150 $\mu\text{J}/\text{cm}^2$ (4CdSe), 320 $\mu\text{J}/\text{cm}^2$ (5CdSe), and 220 $\mu\text{J}/\text{cm}^2$ (3CdS/4CdSe/3CdS).

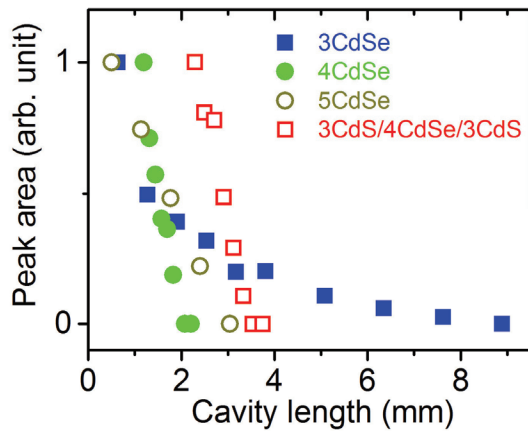


Figure S6. Cavity-length-dependent lasing peak area showing the disappearance of lasing when the cavity length was increased.

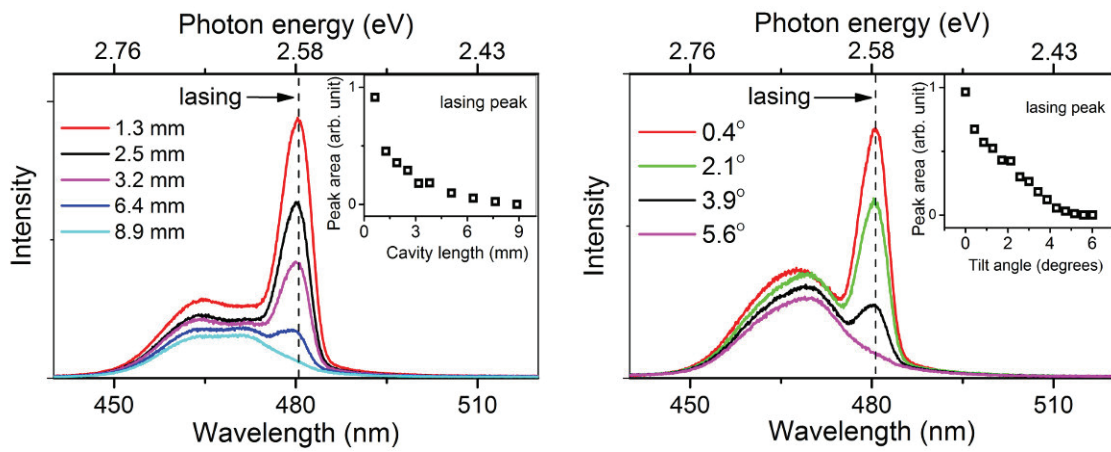


Figure S7. Emission spectra from 3CdSe NPLs in optical cavities by changing the cavity length (left), and tilting the cavity angle (right). Excitation is at 400 nm. The dash lines indicate lasing peaks. Lasing peaks decreased before disappearing when the cavity length increased or the cavity tilted, while spontaneous emissions were always present.

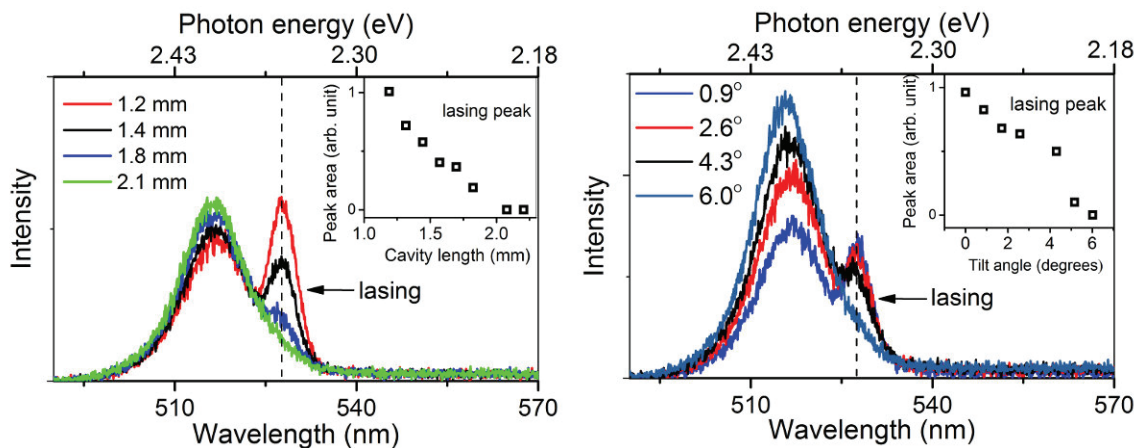


Figure S8. Emission spectra from 4CdSe NPLs in optical cavities by changing the cavity length (left), and tilting the cavity angle (right). Excitation is at 400 nm. The dash lines indicate lasing peaks. Lasing peaks decreased before disappearing when the cavity length increased or the cavity tilted, while spontaneous emissions were always present.

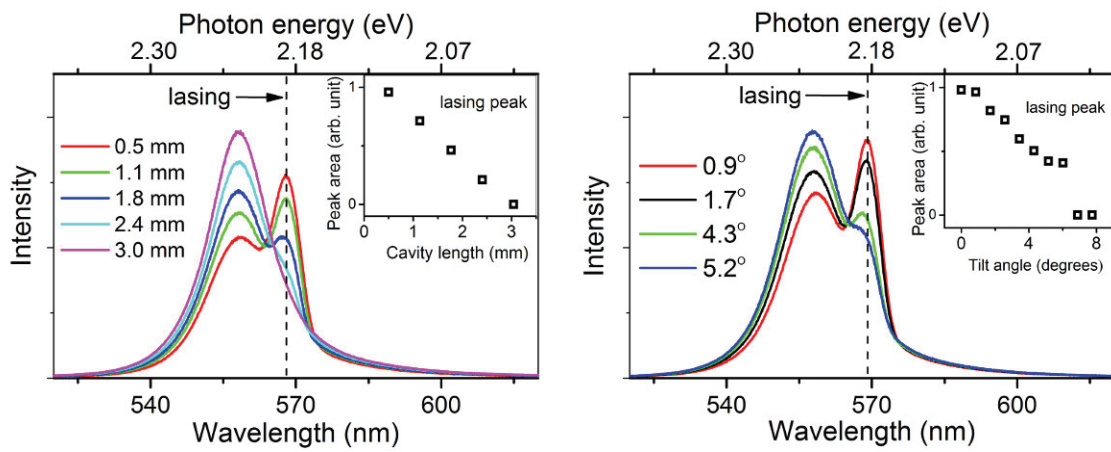


Figure S9. Emission spectra from 5CdSe NPLs in optical cavities by changing the cavity length (left), and tilting the cavity angle (right). Excitation is at 400 nm. The dash lines indicate lasing peaks. Lasing peaks decreased before disappearing when the cavity length increased or the cavity tilted, while spontaneous emissions were always present.

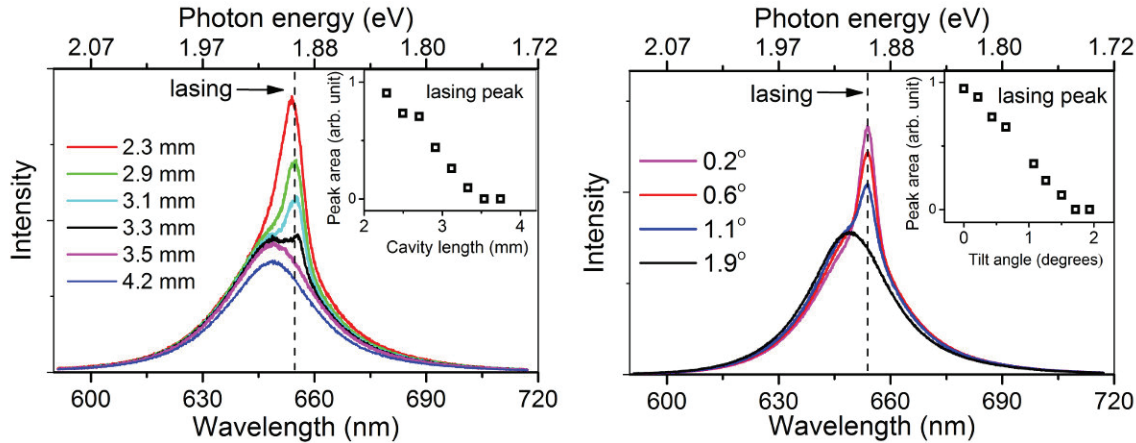


Figure S10. Emission spectra from 3CdS/4CdSe/3CdS NPLs in optical cavities by changing the cavity length (left), and tilting the cavity angle (right). Excitation is at 400 nm. The dash lines indicate lasing peaks. Lasing peaks decreased before disappearing when the cavity length increased or the cavity tilted, while spontaneous emissions were always present.

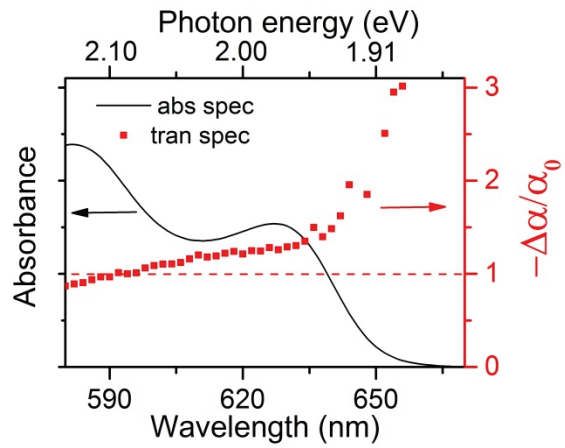


Figure S11. Absorption and transient spectra (calculated as $-\Delta\alpha/\alpha_0$) of 3CdS/4CdSe/3CdS NPLs in hexane. The pump fluence was $660 \mu\text{J}/\text{cm}^2$. Optical gain refers to the spectral region where $-\Delta\alpha/\alpha_0$ is greater than 1. The gain bandwidth is about 0.22 eV.

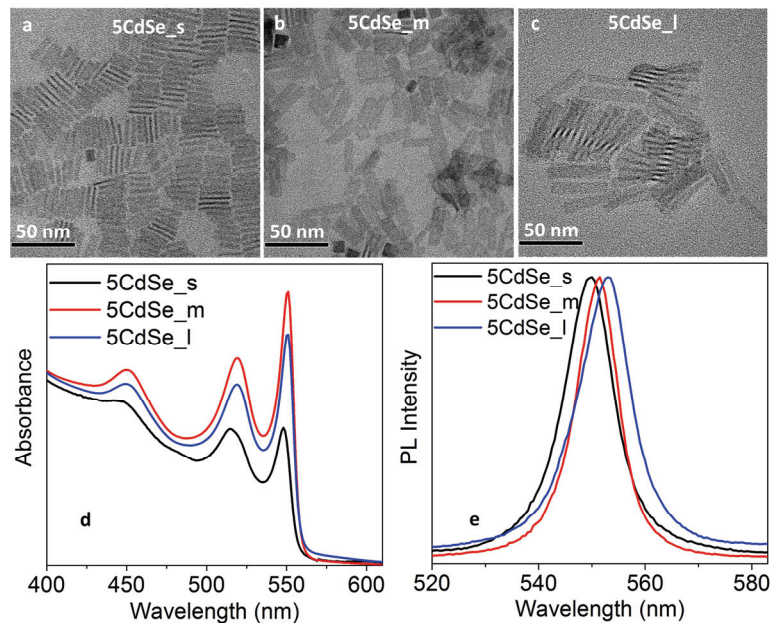


Figure S12. Transmission electron microscope images of (a) 5CdSe_s, (b) 5CdSe_m, (c) 5CdSe_l, with lengths of 25 ± 3 , 29 ± 4 , and 39 ± 5 nm, respectively. The widths of 5CdSe_s, 5CdSe_m, and 5CdSe_l are 7 ± 2 nm, 8 ± 1 nm, and 10 ± 1 nm, respectively. (d) Absorption spectra of 5CdSe_s, 5CdSe_m, and 5CdSe_l NPLs in hexane solutions. (e) Emission spectra of 5CdSe_s, 5CdSe_m, and 5CdSe_l NPLs in hexane solutions.

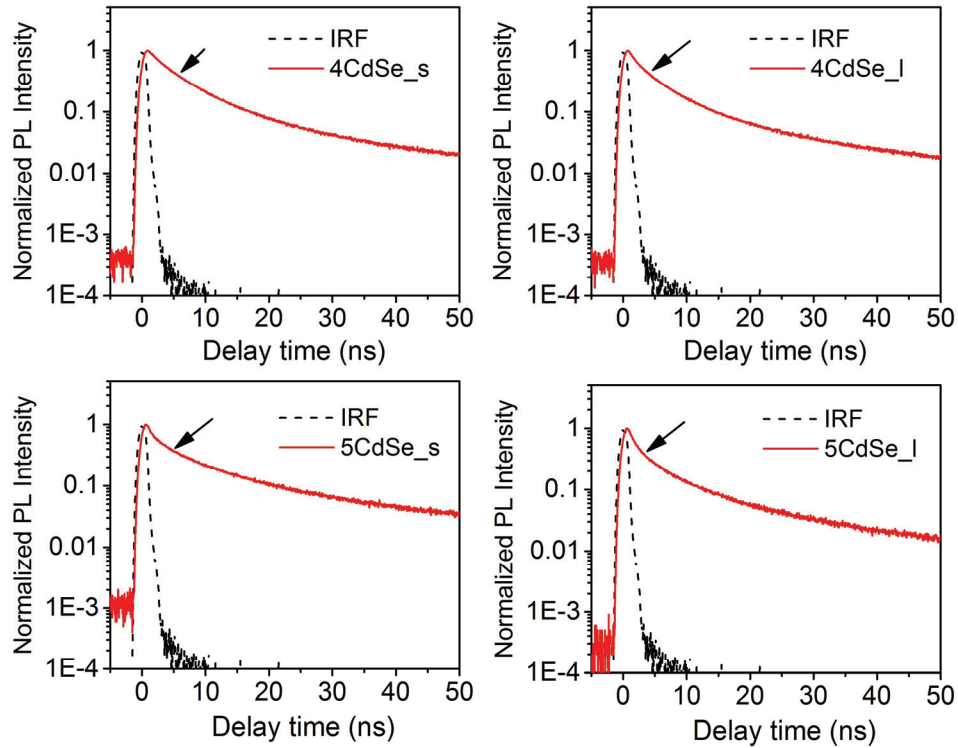


Figure S13. Photoluminescence decay of 4CdSe_s, 4CdSe_l, 5CdSe_s, and 5CdSe_l NPLs in hexane solutions. The instrument response time is about 1.3 ns. Arrows point to the times when the PL signals decay by $1/e$ (63%). The single-exciton lifetimes ($1/e$ time) for all the NPLs are between 3 and 6 ns which is at least 10-fold longer than measured biexciton decay time.

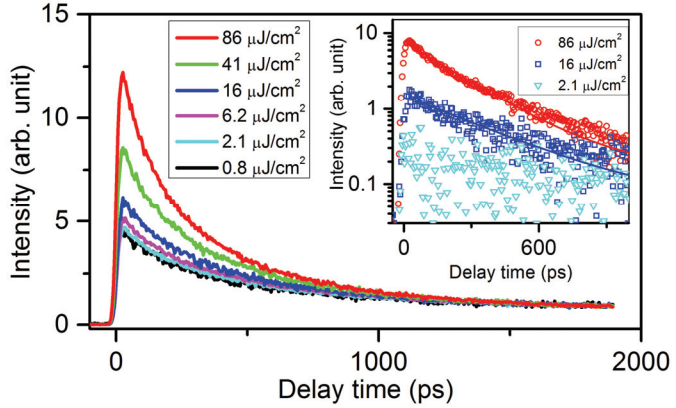


Figure S14. Early-time pump fluence-dependent emission dynamics of 4CdSe NPLs. The dynamics are normalized at about 1.9 ns. The inset shows Auger recombination dynamics at each pump fluence after subtracting the single exciton dynamics at $0.8 \mu\text{J}/\text{cm}^2$. The negligible Auger amplitude (cyan dots) at $2.1 \mu\text{J}/\text{cm}^2$ is indicative of the single exciton dynamics at $0.8 \mu\text{J}/\text{cm}^2$.

Given the fluence F and the absorption cross-section σ , we calculate the average number of excitons per nanoplatelet right after the excitation as:¹

$$\langle N_0 \rangle = \frac{(F / \hbar\omega)\sigma}{1 + (F / F_0)},$$

where F_0 is the saturation fluence, determined to be $90 \mu\text{J}/\text{cm}^2$ in Ref. 1. At pump fluences of $0.8 \mu\text{J}/\text{cm}^2$ and $2.1 \mu\text{J}/\text{cm}^2$, the average number of excitons per NPL is below 0.1 (Figure S14 A), which means the fraction of biexcitons does not exceed 5% based on the Poisson distribution.

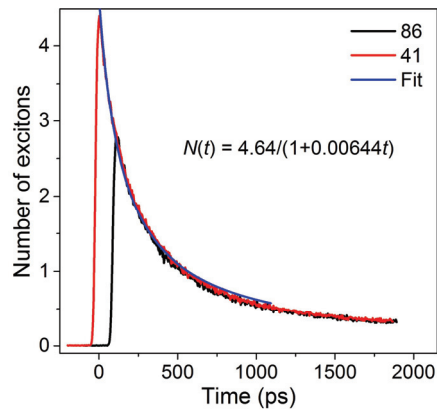


Figure S15. PL decay traces for the highest two fluences in Figure S14 translated horizontally to superimpose onto each other. Further analysis shows that at high pump powers the system obeys the second-order kinetics determined by the volume density of excitons rather than exciton population per NPL (Ref. 1). For this case, the time-dependent exciton population can be expressed as $N = N_0 / (1 + kN_0 t)$, where N is the number of excitons per NPL at time t , N_0 is the initial number of excitons per NPL, and k is second-order rate constant. The value for k in our case is 0.00139 exciton⁻¹s⁻¹, which is close to 0.00125 exciton⁻¹s⁻¹ reported in Ref. 1. The lifetime in the second-order kinetics does depend on the initial number of excitons, and for the highest fluence used in our work, it equals 267 ps. The two-exciton recombination rate (the slope of the curve at $\langle N \rangle = 2$) or $k \cdot 2^2 = 5.5$ excitons/ns.

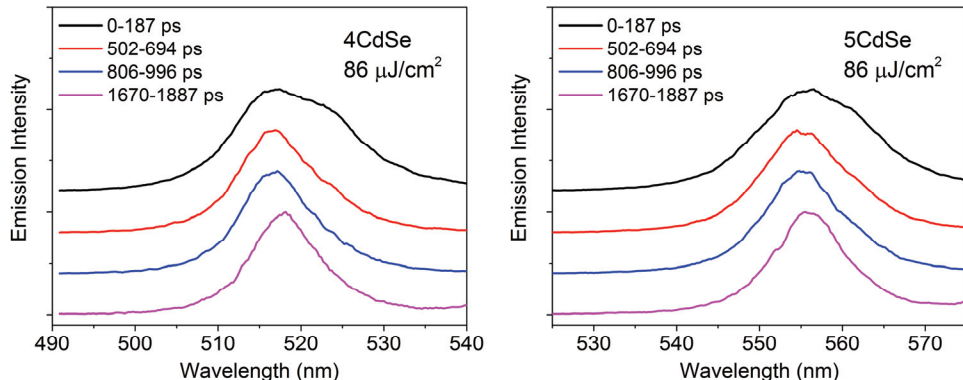


Figure S16. Time-resolved emission spectra of 4CdSe and 5CdSe nanoplates. The pump fluence is 86 $\mu\text{J}/\text{cm}^2$.

Supplementary reference:

1. Baghani, E.; O'Leary, S. K.; Fedin, I.; Talapin, D. V.; Pelton, M. *J. Phys. Chem. Lett.* **2015**, 6, 1032-1036.